JOURNAL OF VIROLOGY, Nov. 1980, p. 440–449
0022-538X/80/11-0440/10$02.00/0

Vol. 36, No. 2

Coronavirus Multiplication Strategy

II. Mapping the Avian Infectious Bronchitis Virus Intracellular RNA Species to the Genome

DAVID F. STERN†* AND S. IAN T. KENNEDY

Department of Biology, University of California, San Diego, La Jolla, California 92093

Avian infectious bronchitis virus, a coronavirus, directs the synthesis of six major single-stranded polyadenylated RNA species in infected chicken embryo kidney cells. These RNAs include the intracellular form of the genome (RNA F) and five smaller RNA species (RNAs A, B, C, D, and E). Species A, B, C, and D are subgenomic RNAs and together with the genome form a nested sequence set, with the sequences of each RNA contained within every larger RNA species (D. F. Stern and S. I. T. Kennedy, J. Virol 34:665–674, 1980). In the present paper, we show by RNase T_1 oligonucleotide fingerprinting that RNA E is also a member of the nested set. Partial alkaline fragmentation of the genome followed by sucrose fractionation, oligodeoxythymidylate-cellulose chromatography, and RNase T_1 fingerprinting gave a partial 3′-to-5′ oligonucleotide spot order. A comparison of the oligonucleotides of each of the five subgenomic RNAs with this spot order established that all of the RNAs are comprised of nucleotide sequences inward from the 3′ end of the genome. This result is discussed in relation to the multiplication strategy both of coronaviruses and of other RNA-containing viruses.

The coronaviruses are enveloped viruses with a positive-stranded RNA genome. They cause a diverse group of diseases in different hosts (13). There is no consensus on the size of the coronavirus genome; however, several studies have resulted in estimated molecular weights ranging between 6×10^6 and 9×10^6 (10, 11, 14, 18).

We have begun characterization of viral RNA species synthesized in chicken embryo kidney (CEK) cells infected with the avian coronavirus infectious bronchitis virus (IBV) as part of our overall investigation of the multiplication strategy of coronaviruses. Recently, we described six major virus-specified RNAs found in IBV-infected cells (16). The species include RNA F, which has the same electrophoretic mobility as the genome, and five smaller RNA species, A, B, C, D, and E, which have apparent molecular weights of 0.8×10^6, 0.9×10^6, 1.3×10^6, 1.5×10^6, and 2.6×10^6, respectively. RNase T_1 oligonucleotide fingerprint analysis of species A, B, C, D, and F and the genome demonstrated that RNA F is the intracellular form of the genome and that RNAs A, B, C, and D are subgenomic RNA species. Since RNAs A to D were shown to be single-stranded, polyadenylated RNAs, they are likely to be viral mRNA's. The oligonucleotide maps of these RNAs also showed that RNAs A, B, C, D, and F (the genome) comprise a nested set; each RNA species contained the sequences found in the smaller RNAs and was included within every larger RNA.

In this report we present the fingerprint of intracellular RNA E, which indicates that this species also belongs to the nested sequence set and that therefore the nested set includes all six RNA species. To enable mapping of the members of this set to the genome, we determined a partial 3′-to-5′ oligonucleotide spot order for the genome. The results demonstrate that all five subgenomic RNA species share a common 3′ end and that all these RNAs extend inward from the 3′ end of the genome. The significance of this finding with respect to the strategies of other positive-stranded RNA viruses is discussed.

MATERIALS AND METHODS

Agarose (type II), sodium ADP, sodium pyruvate, and cysteine-hydrochloride hydrate were purchased from Sigma Chemical Co. L-α-Glycerophosphate and βNAD$^+$ were obtained from Boehringer Mannheim Biochemicals.

Oligodeoxythymidylate [oligo(dT)]-cellulose (type 3) was purchased from Collaborative Research Inc., and Sephadex G-75 was purchased from Pharmacia Fine Chemicals, Inc. Carrier-free $^{32}P_i$ (285 Ci/mg) was supplied by ICN. Autoradiography was performed by using Kodak X-Omat R film and Cronex Lightning-Plus intensifying screens. ACS scintillation fluid was purchased from Amersham Corp.

^{32}P-labeled *Chlamydomonas* RNA was a gift from

† Present address: Tumor Virology Laboratory, The Salk Institute, San Diego, CA 92138.

Manuel Ares. Phenol, ethanol, and ether were redistilled before use. All other reagents were the highest grade commercially available.

Yeast tRNA (type X) was obtained from Sigma Chemical Co. and purified as described previously (16). Glycogen was obtained from Calbiochem-Behring Corp., dissolved at 20 mg/ml in 10 mM Tris, pH 7.2, 500 mM NaCl, and 10 mM $MgCl_2$, and digested with 50 μg of DNase (type BAPF, Worthington Biochemicals Corp.) per ml at 37°C for 1 h. Proteinase K (Merck & Co., Inc.) was added to give a concentration of 250 μg/ml. The solution was incubated at 50°C for 20 min and then at 25°C for 20 min; it was then extracted once with phenol-chloroform (1:1, vol/vol, saturated with 50 mM Tris, pH 7.4, 100 mM NaCl, and 1 mM EDTA [TNE]). Glycogen was precipitated from the aqueous phase with 2.5 volumes of redistilled EtOH at −20°C. The material was recovered from alcohol by centrifugation, dissolved in 0.2 M KOH, and incubated at 37°C for 18 h. After neutralization with acetic acid, the material was extracted once with phenol-chloroform, alcohol precipitated as before, recovered by centrifugation, dissolved in water, and stored at a concentration of 20 mg/ml at −20°C.

Enzymes. Calf intestinal alkaline phosphatase [supplied as a suspension in 3.2 M $(NH_4)_2SO_4$] was obtained from Boehringer Mannheim Biochemicals. The enzyme was recovered by centrifugation at 12,000 × *g* for 5 min, dissolved in 50 mM Tris, pH 8.0, containing 250 mM NaCl, and purified by passage over a Sephadex G-75 column which was eluted with the sample buffer. Active fractions were pooled, and the enzyme was stored at a concentration of 5 U/ml in 25 mM Tris, pH 8.0, 125 mM NaCl, and 50% glycerol at −20°C. To assay phosphatase activity, 1 μl of each column fraction was combined with 9 μl of 11 mM Tris, pH 8.0, containing 3×10^6 cpm of [γ-^{32}P]ATP (250 Ci/mmol) and incubated at 37°C for 30 min. The reaction was monitored by thin-layer chromatography on polyethyleneimine plates (Machery-Nagel and Co.) developed with 0.75 M potassium phosphate adjusted to pH 3.5 with phosphoric acid. Sankyo RNase T_1 was purchased from Calbiochem-Behring Corp., and T_4 polynucleotide kinase was purchased from P-L Biochemicals, Inc. Rabbit muscle glycerophosphate dehydrogenase (60 U/mg, 2 mg/ml), rabbit muscle triosephosphate isomerase (5,000 U/mg, 2 mg/ml), rabbit muscle glyceraldehyde-3-phosphate dehydrogenase (80 U/mg, 10 mg/ml), yeast 3-phosphoglycerate kinase (450 U/mg, 10 mg/ml), and rabbit muscle lactate dehydrogenase (550 U/mg, 5 mg/ml) were obtained from Boehringer Mannheim Biochemicals as suspensions in 3.2 M $(NH_4)_2SO_4$.

Cells and viruses. Plaque-purified Beaudette strain (strain 42) IBV was propagated in primary CEK cells as described previously (16).

Preparation of intracellular RNA E for fingerprinting. CEK cells in five 150-mm tissue culture dishes were infected with IBV at a multiplicity of infection of about 30. Intracellular RNA was labeled with $^{32}P_i$ in the presence of actinomycin D, and cytoplasmic nuclei acids were extracted with sodium dodeylsulfate (SDS)-phenol-chloroform and ethanol precipitated exactly as described before (16).

The nucleic acids were recovered from alcohol by centrifugation, dried in vacuo over $CaCl_2$, dissolved in 300 μl of 1/10 TNE containing 5% sucrose and 0.002% bromophenol blue, and applied to a horizontal 1.2% agarose slab gel for electrophoresis as described previously (12). After electrophoresis, the gel bands corresponding to intracellular RNA E were located by autoradiography of the wet gel and excised. RNA was recovered from the gel slices as described before (16).

Preparation of virion RNA. Preparation of $^{32}P_i$-labeled IBV in CEK cells and purification of the virus have been described (16). Briefly, CEK cells were infected at a multiplicity of infection of 1.5 and incubated in the presence of $^{32}P_i$, and virions were subsequently purified by equilibrium banding in sucrose gradients.

One additional step was performed for the genome fingerprint in Fig. 1c. Virus in the clarified culture fluid was concentrated by pelleting before equilibrium banding. Portions (20 ml) of clarified fluid were layered onto 6 ml of 30% (wt/vol) sucrose prepared in TNE and centrifuged at 64,000 × *g* for 2.5 h at 4°C in a type 30 rotor. The pellets were suspended in 2 ml of TNE, and virus was purified by equilibrium banding as described previously (16) except that the entire 2-ml suspension was layered on a single 34-ml sucrose gradient for equilibrium sedimentation.

Virion RNA was extracted with proteinase K-SDS and phenol-chloroform. In spot order experiment 1, virion RNA was extracted and layered directly on sucrose velocity gradients to enable selection of high-molecular-weight virion RNA. Total virion RNA was extracted and used in all other experiments. Both methods have been described in detail previously (16).

Fragmentation of RNA with alkali. RNA to be degraded was recovered from ethanol and suspended in 48 μl of TLE buffer (50 mM Tris, pH 7.4, 100 mM LiCl, and 1 mM EDTA). Then 48 μl of freshly prepared 2 M Na_2CO_3 was added to give a final concentration of 1 M Na_2CO_3. For spot order experiment 1 (mild treatment), the solution was incubated for 30 s at 20°C and the reaction was terminated by neutralization with 16 μl of glacial acetic acid. For spot order experiment 2 (harsh treatment), the sample was split into two 24-μl portions; one was incubated at 20°C for 2 min, and the other was incubated at 37°C for 3 min. The reactions were terminated with acetic acid as before, and the portions were combined. Then 100 μl of TLES (TLE with 0.1% SDS) was added to the experiment 1 sample and 300 μl was added to the experiment 2 sample in preparation for velocity sedimentation.

Sedimentation of fragmented RNA. In spot order experiment 1, the degraded RNA was applied to an 11-ml linear 15 to 30% (wt/vol) sucrose gradient prepared in TLES and centrifuged at 150,000 × *g* for 4 h at 10°C in an SW41 rotor. In experiment 2, fragmented RNA was layered on an 11.6-ml linear 5 to 25% (wt/vol) sucrose gradient prepared in TLES. ^{32}P-labeled *Chlamydomonas* RNA was layered onto a parallel gradient, and the gradients were centrifuged at 150,000 × *g* for 6 h at 10°C in an SW41 rotor. After centrifugation, the gradients were fractionated and portions were counted by scintillation spectrometry. Fractions were pooled as described in Fig. 3 and stored at −70°C before oligo(dT)-cellulose selection.

Oligo(dT)-cellulose chromatography. Four molar LiCl was added to each pool to give a final concentration of 0.3 M LiCl, and the samples were chromat-

ographed on oligo(dT)-cellulose as described previously (5). The 3.0-ml eluate containing polyadenylated RNA was made 0.3 M in NaCl, 400 μg of glycogen carrier was added, and nucleic acid was precipitated with 2.5 volumes of redistilled ethanol at −20°C.

Kinase labeling and fingerprinting of RNase T_1 oligonucleotides. (i) RNase T_1 digestion. Nucleic acid was recovered from the samples by centrifugation and dissolved in 5 μl of 20 mM Tris, pH 7.4. Then 5 μl of a 1-mg/ml solution of RNase T_1 was added, and the samples were incubated at 37°C for 30 min. Forty microliters of water was added, and the samples were extracted once with phenol-chloroform (1:1, vol/vol, saturated with water) in 500-μl Eppendorf microtubes. The organic phase was then extracted with an additional 20 μl of water, and the combined aqueous phases were extracted once with redistilled ether. Finally, the aqueous phase was lyophilized.

(ii) Alkaline phosphatase treatment. The dried oligonucleotides were dissolved in 20 μl of Tris, pH 8.0; 5 μl (25 mU) of purified calf alkaline phosphatase was added, and the samples were incubated at 37°C for 1 h. Then 25 μl water was added, and the samples were extracted with phenol-chloroform and ether and lyophilized exactly as described above.

(iii) Kinase labeling. For each sample, 1 mCi of [γ-^{32}P]ATP, prepared as described below, was dried in vacuo over $CaCl_2$ in a 500-μl Eppendorf microtube. The phosphatase-treated oligonucleotides were dissolved in 20 μl of 50 mM Tris, pH 7.6, 10 mM $MgCl_2$, and 5 mM dithiothreitol and transferred to the tubes containing the lyophilized ATP. T_4 polynucleotide kinase (3.5 U) was added to each tube, and the samples were incubated at 37°C for 1 h and extracted with phenol-chloroform and ether as described above. Then 100 μg of purified tRNA was added, and the kinase-treated oligonucleotides were precipitated with 3 volumes of redistilled ethanol at −20°C overnight.

(iv) Oligonucleotide fingerprinting. The oligonucleotides were recovered from ethanol by centrifugation, and the pellets were washed twice with 70% ethanol containing 50 mM NaCl and dried in vacuo over $CaCl_2$. Separation of the oligonucleotides by two-dimensional polyacrylamide gel electrophoresis has been described previously (8, 16). The gels were autoradiographed with intensifying screens at −70°C for 12 to 48 h.

Preparation of [γ-^{32}P]ATP. The method of Walseth and Johnson (17) was used with the following modifications. (i) The concentrations of triosephosphate isomerase and 3-phosphoglycerate kinase in the reaction mixture were increased threefold and twofold, respectively. (ii) The progress of the reaction was monitored by removing 0.5-μl portions from the reaction mixture and analyzing these by thin-layer chromatography on polyethyleneimine plates as described above. (iii) After the reaction (for 30 min at room temperature), the mixture (100 μl) was made to 1 ml with water and extracted once with phenol-chloroform (1:1, vol/vol, water saturated) and once with redistilled ether, and [γ-^{32}P]ATP was stored in 50% ethanol at −20°C.

RESULTS

RNase T_1 oligonucleotide fingerprint of intracellular RNA E.

We recently reported that IBV directs the synthesis of six intracellular RNA species (A, B, C, D, E, and F; 16). RNAs A, B, C, D, and F (the intracellular form of the genome) were shown by RNase T_1 fingerprint analysis to form a nested sequence set. To determine the sequence relationship between RNA E and the other intracellular RNA species, we purified ^{32}P-labeled RNA E by preparative agarose gel electrophoresis and fingerprinted it (Fig. 1b). The polyadenylate [poly(A)] tract is visible as a streak in the upper left-hand corner. The large circular mark located to the right of the streak is an artifact and was not seen in other fingerprints of RNA E (data not shown). Comparison of the fingerprint to the genome fingerprint in Fig. 1c reveals that all spots in RNA E were also present in the genome, establishing that RNA E is a subgenomic species. Moreover, RNA E contained all of the oligonucleotides in the fingerprint of RNA D (Fig. 1a) as well as an additional 22 oligonucleotides which are indicated by arrowheads in Fig. 1. Thus, RNA E is also a member of the nested set, which therefore includes all six intracellular RNA species previously described.

The fingerprint of RNA E included one spot not found in the previously published fingerprint of the genome (16). This spot, marked P in Fig. 1, sometimes appeared in fingerprints of the intracellular genome (RNA F) as well as virion RNA (data not shown). Since the intensity of the spot is quite variable, it is possible that the spot is an incomplete T_1 digestion product.

Fingerprinting of kinase-labeled oligonucleotides. We chose to use kinase-labeled T_1 oligonucleotides for the spot order experiments because the high specific activity resulting from this labeling method greatly reduces the amount of viral RNA required for fingerprint analysis. Figure 2b shows a kinase fingerprint of virion RNA prepared as described in Materials and Methods. The RNA used for this fingerprint was a portion of the RNA used in spot order experiment 1 (see below). All of the spots in the in vivo-labeled genome RNA fingerprint in Fig. 2a were also found in the kinase fingerprint (Fig. 2b); however, some spots in the kinase fingerprint (for example, those marked U and V) were less radioactive than their counterparts labeled in vivo. The differences were reproducible and could be due to lower efficiency of labeling by polynucleotide kinase possibly resulting from secondary structure constraints or reduced recovery of these oligonucleotides during the kinase fingerprinting procedure.

Genome oligonucleotide spot order. To enable mapping of the intracellular RNA species to the genome, we determined a partial genome

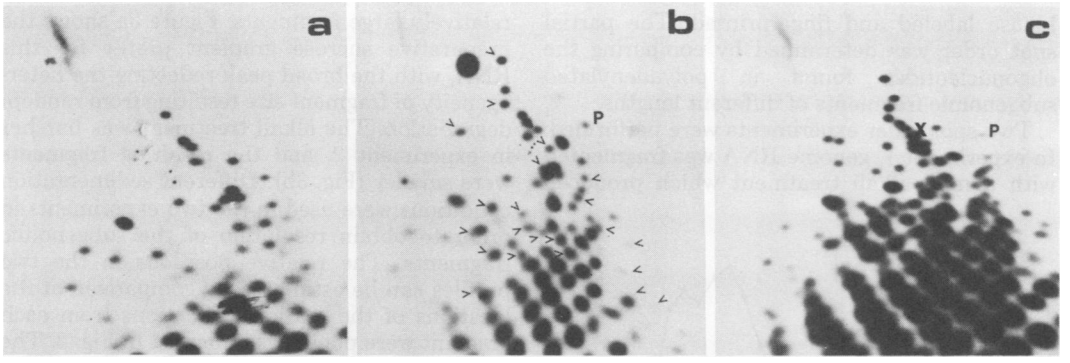

FIG. 1. *RNase T_1 fingerprints of intracellular RNAs D and E and the IBV genome. The fingerprint of RNA D (purified by polyacrylamide gel electrophoresis) has been published previously (16). To prepare intracellular RNA E, five 150-mm petri dish CEK cultures were infected with IBV at a multiplicity of infection of about 30 and labeled with $^{32}P_i$ in the presence of actinomycin D. Nucleic acid extracts were prepared; then RNA E was purified by agarose gel electrophoresis (see Materials and Methods) and recovered by adsorption to and elution from hydroxylapatite (16). About 90,000 cpm of RNA was fingerprinted as described previously (8, 16). In this and all subsequent fingerprints, electrophoresis was from left to right in the first dimension and from top to bottom in the second. Autoradiography was for 5 days at −70°C with an intensifying screen. $^{32}P_i$-labeled genomic RNA was purified from six IBV-infected 150-mm petri dish CEK cultures as reported previously (16) with the modification described in Materials and Methods. About 480,000 cpm of RNA was fingerprinted and autoradiographed for 6 days at −70°C with an intensifying screen. X and B indicate the positions of the xylene cyanol FF and bromophenol blue tracker dyes. (a) RNA D; (b) RNA E; (c) genomic RNA. The significance of the lettered and arrowed spots is discussed in the text.*

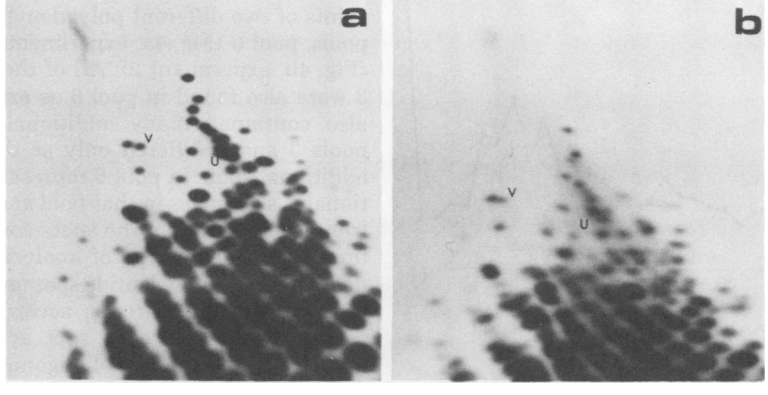

FIG. 2. *RNase T_1 fingerprints of in vivo-labeled and kinase-labeled IBV genomic RNA. The fingerprint of genomic RNA labeled in vivo (a) is the same fingerprint as is shown in Fig. 1c. Genomic RNA to be labeled with polynucleotide kinase was prepared from seven IBV-infected 150-mm petri dish CEK cultures which were incubated with $^{32}P_i$ after adsorption. Virions were purified, nucleic acids were extracted, and high-molecular-weight RNA was selected on sucrose velocity gradients as described in Materials and Methods. Five-sixths of the RNA was used in spot order experiment 1. The remaining RNA was kinase labeled and fingerprinted as described in Materials and Methods and autoradiographed for 6 h at room temperature. (a) In vivo-labeled genomic RNA; (b) kinase-labeled genomic RNA. The significance of the lettered spots is discussed in the text.*

3′-to-5′ RNase T_1 oligonucleotide spot order. The experiment was performed by purifying ^{32}P-labeled genomic RNA from virus particles, fragmenting the RNA with alkali, separating the fragments according to size by sucrose velocity sedimentation, and isolating polyadenylated RNA fragments from each size class by oligo(dT)-cellulose chromatography. This method generates a series of pools of subgenomic fragments all containing the genome poly(A) (which we assumed to be uniquely at the 3′ end of the genome) and extending inward for increasing lengths from the 3′ end. RNase T_1 oligonucleotides derived from each fragment pool were

kinase labeled and fingerprinted. The partial spot order was determined by comparing the oligonucleotides found in polyadenylated subgenomic fragments of different lengths.

Two spot order experiments were performed. In experiment 1, genome RNA was fragmented with a mild alkali treatment which produced relatively large fragments. Figure 3a shows the preparative sucrose gradient profile for this RNA, with the broad peak reflecting the heterogeneity of fragment size resulting from random degradation. The alkali treatment was harsher in experiment 2, and the resulting fragments were smaller (Fig. 3b). Different sedimentation conditions were used in the two experiments in order to obtain resolution of the subgenomic fragments. The relative positions in the two profiles can be estimated by comparison of the locations of the markers. Fractions from each gradient were pooled as indicated in Fig. 3. The pools used to derive the spot order are numbered consecutively from 1 to 7 in order of increasing size as determined from the oligonucleotide complexity of the fingerprints. This size order is colinear with the relative positions of the pooled fractions on the gradients. The two pools marked 5 in Fig. 3a and 3b yielded virtually identical fingerprints, and both pools marked 4 also appeared similar.

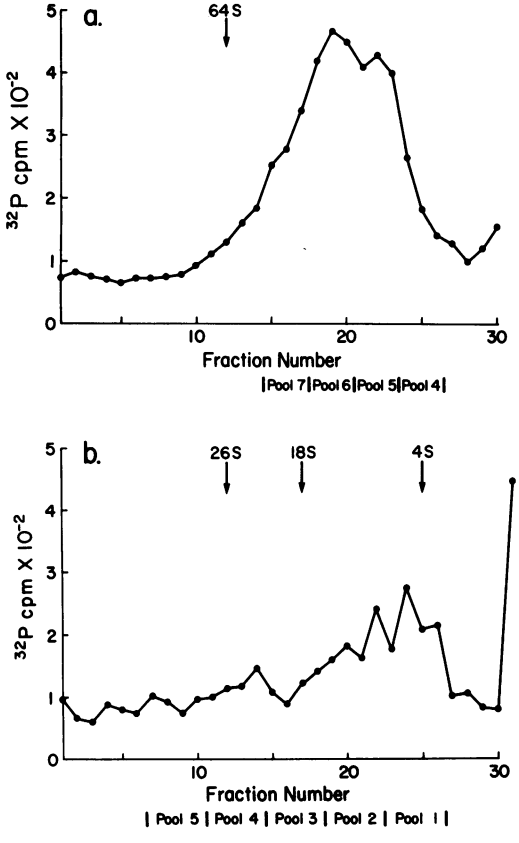

FIG. 3. *Sedimentation of genomic RNA fragmented with alkali. RNA for spot order experiment 1 was prepared as described in the legend to Fig. 2. RNA for spot order experiment 2 was prepared in the same way except that total virion RNA was used. In both experiments, the RNA was recovered from ethanol, partially degraded with alkali, and subjected to velocity sedimentation as described in Materials and Methods. Different sedimentation conditions were used in the two experiments. Sedimentation was from right to left. The arrow in panel a (experiment 1) indicates the location of the peak of undegraded genome RNA (64S; 10) centrifuged under identical conditions in previous experiments; the arrows in panel b (experiment 2) indicate the positions of 4S, 18S, and 26S peaks of ^{32}P-labeled Chlamydomonas RNA sedimented in a parallel gradient. Fractions were pooled as shown in preparation for oligo(dT)-cellulose chromatography and subsequent fingerprint analysis.*

Polyadenylated RNA from each fragment pool was selected by oligo(dT)-cellulose chromatography, digested with RNase T_1, kinase labeled, and fingerprinted as described in Materials and Methods. Figure 4 shows the fingerprints of two different polyadenylated fragment pools, pool 6 (Fig. 4a, experiment 1) and pool 3 (Fig. 4b, experiment 2). All of the spots in pool 3 were also found in pool 6 as expected; pool 6 also contained many additional spots. Since pools 3 and 6 differed only at the 5′ end, the additional spots in pool 6 represented the additional 5′ sequences in that pool and were further from the 3′ end than the spots common to both fingerprints. This type of analysis was used to deduce the oligonucleotide spot order. The spots were divided into groups according to which pool first included each spot at its usual full intensity. Seven groups of oligonucleotides were defined in this way, with each group consisting of the 5′ oligonucleotides unique to the corresponding pool (see Fig. 7a). For example, pool 1 contained the smallest subgenomic fragment, so the oligonucleotides in that pool were those closest to the 3′ end of the genome and were designated group 1. The next-larger fragments were found in pool 2, which contained the group 1 oligonucleotides as well as a new set. Since pools 1 and 2 differed only at the 5′ end, the oligonucleotides specific to pool 2 were located to the 5′ side of the group 1 oligonucleotides, and these additional oligonucleotides were termed group 2. The spot order data were internally consistent in the sense that each fingerprint included all of the spots found in fingerprints of smaller pools. The fragments within a pool were somewhat heterogeneous in size, and the poor resolution of

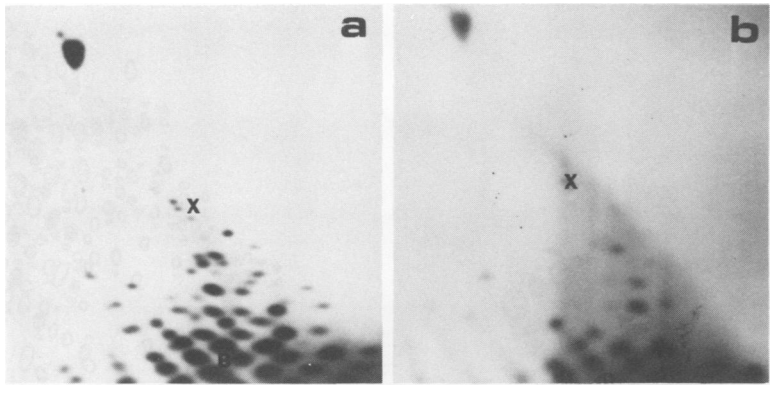

FIG. 4. *RNase T_1 fingerprints of pools 6 (a) and 3 (b). Polyadenylated RNA fragments from pool 6 (spot order experiment 1) and pool 3 (spot order experiment 2) were digested with RNase T_1, kinase labeled, and fingerprinted as described in Materials and Methods. Autoradiography was for 15 and 48 h, respectively, at 4°C with intensifying screens. X and B indicate the locations of the xylene cyanol FF and bromophenol blue tracker dyes.*

sucrose gradients resulted in some overlap between neighboring pools. Often a spot would appear faintly in one pool and darker in fingerprints of successive pools. A spot was consequently assigned to the group corresponding to the pool where that oligonucleotide first appeared with the relative intensity observed in kinase fingerprints of the genome (see Fig. 2) as estimated by visual inspection of the fingerprints. Group 8 consisted of spots that were not yet at full intensity in pool 7 and therefore were located 5′ to the group 7 oligonucleotides. It should be noted that some of the T_1 oligonucleotides, especially those found near the bromophenol blue tracker dye, could occur more than once in the genome. The group to which each of these spots was assigned indicates the location on the genome of the most 3′ of the oligonucleotides comigrating to that position on the genome fingerprint.

A fingerprint of the genome is diagramed in Fig. 5, with numbers indicating the group to which each spot was assigned. The group number increases with increasing distance of the oligonucleotide from the 3′ end. A number of spots remain unmarked. These oligonucleotides were not seen in any of the spot order pools and are presumably located closer to the 5′ end of the genome than any polyadenylated fragments examined. Alkali treatment itself did not eliminate any spots, since genome RNA degraded with alkali and not subjected to oligo(dT) selection yielded a kinase fingerprint containing all of the spots normally found in the genome (data now shown).

We compared the partial spot order with the T_1 oligonucleotide content of the intracellular RNA species. Figure 6 shows diagrammatically

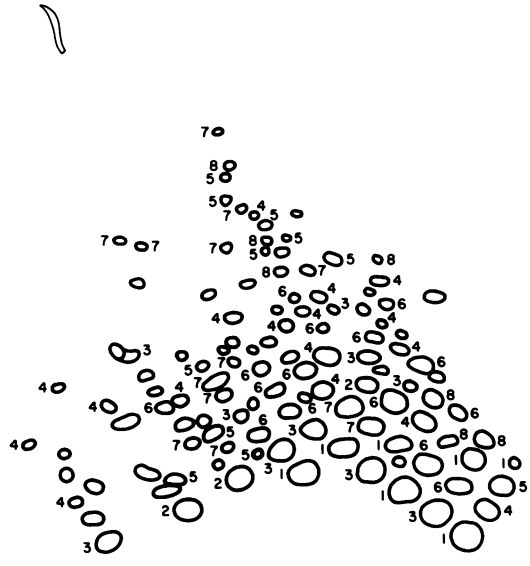

FIG. 5. *Oligonucleotide spot order assignments. A RNase T_1 fingerprint of the IBV genome published previously (16) is diagramed. The numbers indicate the spot order group to which each oligonucleotide belongs, determined as discussed in the text.*

the spot order grouping pictured in Fig. 5 superimposed upon the fingerprints of the intracellular RNA species published in this paper and previously (16). The panels are arranged in order of increasing size of the RNAs, with the oligonucleotides found first in each RNA species filled in and those also occurring in smaller RNAs cross-hatched. The group numbers of the spots are also indicated. The general pattern which emerged is that each intracellular RNA included all of the spots found in some spot

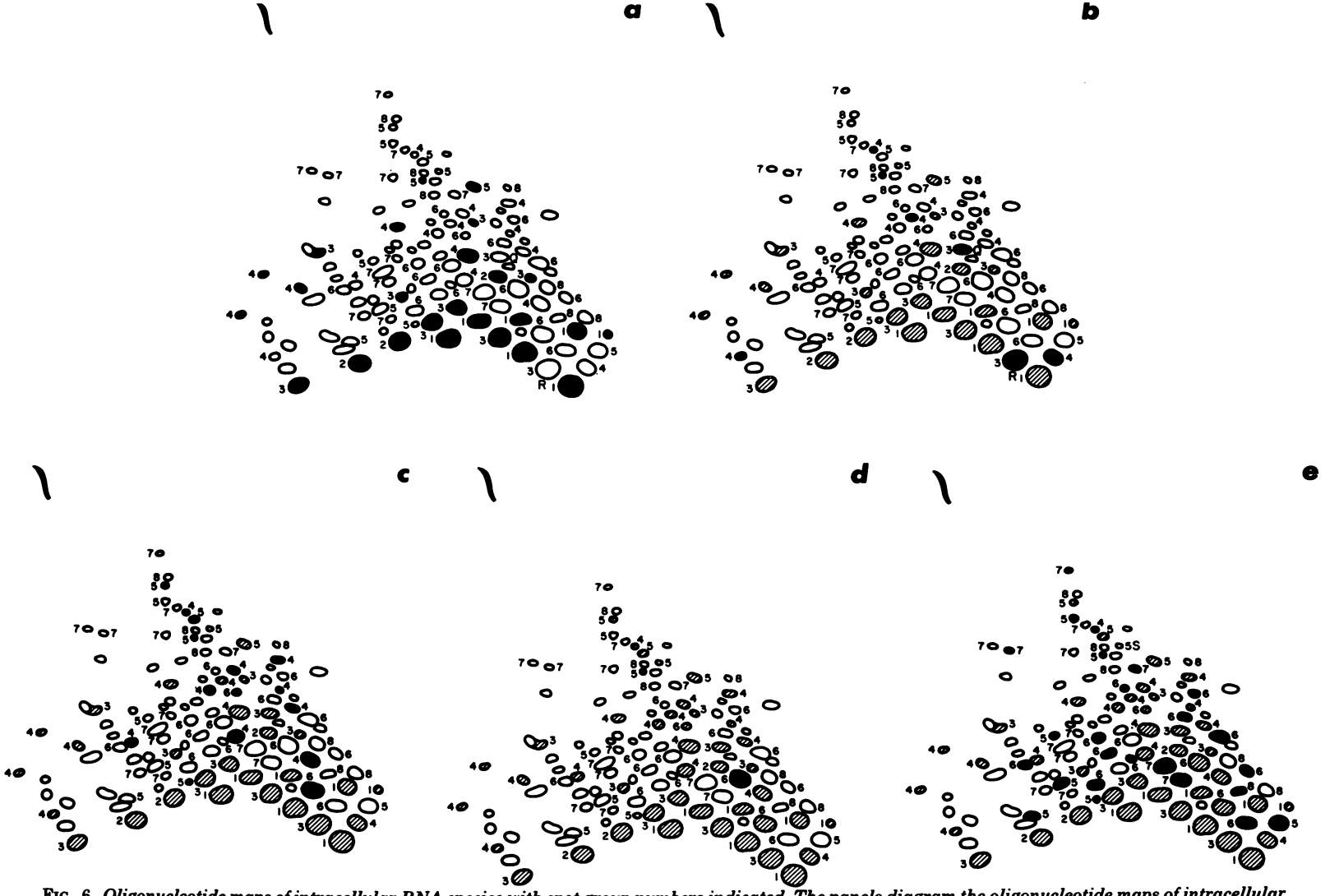

FIG. 6. *Oligonucleotide maps of intracellular RNA species with spot group numbers indicated. The panels diagram the oligonucleotide maps of intracellular RNA species A to E published in this report (RNA E) and previously (species A to D; 16). The panels are arranged in order of increasing size of the intracellular RNA species. The oligonucleotides occurring first in each species are filled in; oligonucleotides also found in smaller RNAs are cross-hatched. The significance of the lettered spots is discussed in the text. Panels a to e represent RNA species A to E, respectively.*

order pools and was wholly contained within larger pools. For example, RNA A (Fig. 6a) contained the spots included in pool 3 and was contained within pool 4. Since pool 3 derives from the 3′ end of the genome, RNA A must include that end. Additional sequences were present in RNA A and not pool 3; since pool 4 did include these spots, it is likely that they represent a simple 5′ extension of pool 3 sequences. Pool 4 spots not found in RNA A would be located 5′ to pool 4 spots which did overlap with RNA A.

The simplest interpretation of our data is diagramed in Fig. 7. The intracellular RNAs could be interpolated into the nested series of spot order fragment pools (Fig. 7a). Since the spot order pools are a nested series of subgenomic fragments differing only at the 5′ end, the intracellular RNAs must form a similar series, with each member of the set sharing a 3′ end common to all the intracellular RNAs including the genome, and with each RNA species bearing a unique 5′ end (Fig. 7b). Since pool 7 includes oligonucleotides not found in RNA E, the pool 7 fragments were slightly longer than species E, which has a molecular weight of 2.6×10^6 (16). Thus, the spot order information pertains to the region extending approximately 3×10^6 daltons from the 3′ end of the genome and so covers slightly less than half of the genome (which has been reported to have a molecular weight of between 6 and 9×10^6 [reviewed in reference 13]).

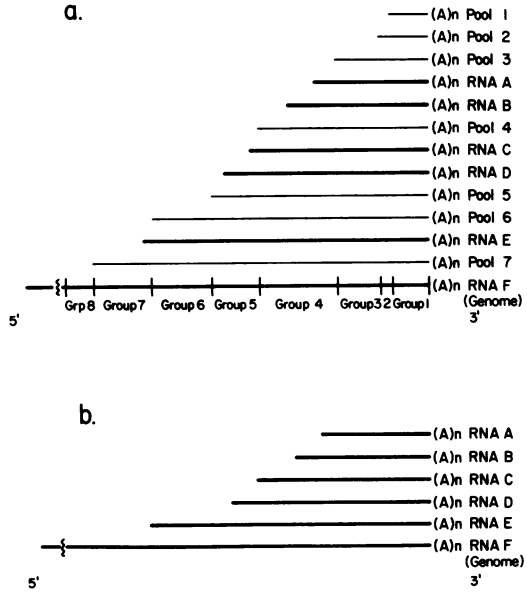

FIG. 7. *Relationships among intracellular RNAs and spot order pools. The intracellular RNA species and spot order pools were mapped with respect to one another as described in the text. They are depicted schematically arranged in order of increasing complexity (not drawn to scale). The relative positions of the oligonucleotide spot groups along the genome are also indicated.*

A few of the spots do not agree precisely with our conclusion. These spots were all assigned to groups immediately adjacent to those which would have been predicted from this scheme. These contradictions may have resulted from experimental error due to three technical problems: the poor resolution of sucrose gradients, the low intensity of certain kinase-labeled spots (U in Fig. 2b), and the subjective visual analysis of the fingerprints. Thus, spots Q and R (Fig. 6a, b) were assigned to group 3 but were not found in RNA A. They did occur in RNA B, which was only slightly larger than species A. The molecular weights of species A and B are 0.8×10^6 and 0.9×10^6, respectively (16), and it is likely that fragments of these two sizes would not be resolved well on sucrose gradients. It would therefore not be surprising if our assignments of spots at this scale resulted in some errors. Only one spot (S, Fig. 6e) deviated from our conclusions by more than one group. This spot was assigned to group 5 but was not found in RNA E, a deviation of two groups. We do not know whether this single deviation is significant. Of the 116 spots characterized, only 9 showed any deviation from the model, and 8 of these 9 spots were misplaced by only one group. We consider these results to be well within the range of experimental error.

DISCUSSION

In a previous report (16), we described six major single-stranded RNA species synthesized in IBV-infected cells in the presence of actinomycin D. Five of the six species (all but RNA E) were analyzed individually by RNase T_1 fingerprinting. This analysis revealed that RNA F is the intracellular genome and the smaller RNAs A, B, C, and D are subgenomic species. The fingerprints further indicated that the five RNAs form an overlapping nested set, with the sequences in each RNA species contained within those of the larger intracellular RNAs and every larger RNA species gaining additional nucleotides congruent with the increase in size. The fingerprint of RNA E presented in Fig. 1 shows that RNA E also fits into the nested set and therefore all six RNAs belong to the nested sequence set.

To enable mapping of the intracellular RNA species to the genome, we determined a partial 3′-to-5′ RNase T_1 oligonucleotide spot order for

the genome. The genome oligonucleotides were assigned to eight groups (Fig. 5 and 7) numbered in order of increasing distance from the genomic poly(A) tract, which we assumed to occur uniquely at the 3′ end of the genome.

Comparison of the partial spot order with oligonucleotide maps of the intracellular RNA species (Fig. 6) established that the RNAs all share a common 3′ end corresponding to the 3′ end of the genome and extend inward from that end for different lengths so that each RNA species bears a unique 5′ end (Fig. 7b). Within the resolution of our data, the intracellular RNA species appear to be colinear with the genome, but we cannot rule out the occurrence of small sequence rearrangements such as might result from RNA splicing. There is no reported precedent, however, for RNA splicing in any wholly cytoplasmic RNA virus system.

Since the intracellular RNA species are polyadenylated single-stranded viral RNAs, we consider them likely to be IBV mRNA's (16). Our own unpublished data and those of others (15) support this idea. In this light, it is of interest to compare the scheme presented in Fig. 7b with strategies utilized by other positive-stranded RNA viruses. Tobacco mosaic virus (TMV) and the alphaviruses Semliki Forest virus and Sindbis virus have been shown to form subgenomic mRNA's (2–4, 6). In these systems, a single subgenomic mRNA is synthesized which extends inward from the 3′ end of the genome, as do the IBV intracellular RNAs. Translation of the genome terminates before the translation initiation site of the subgenomic mRNA so that there is no overlap between the products translated from these two overlapping mRNA's. The translation initiation site expressed in the subgenomic mRNA is not expressed in translation of the genome. This finding supports the hypothesis that internal translation initiation does not occur in eucaryotes (7). The alphaviruses illustrate one other feature common to many positive-stranded viruses. The primary translation products of the genome and the subgenomic mRNA are polyprotein precursors which are processed to form the nonstructural and structural proteins, respectively. This system permits coordinate control of the relative synthesis of these two groups of proteins.

Influenza virus, which has a segmented genome of negative polarity, synthesizes two mRNA's from genome segment 8 which code for polypeptides NS_1 and NS_2. A recent report (9) indicates that these mRNA's overlap in the same way as the IBV intracellular RNAs, with the smaller NS_2 mRNA corresponding to the 3′ terminal portion of the NS_1 mRNA. Interestingly, the results suggest that the two polypeptides may be translated in part from a common region, and the lack of homology between the two proteins may indicate that this region is translated in two different reading frames.

By analogy with TMV and the alphaviruses, one might expect a nonoverlapping translation scheme for IBV whereby only the 5′ region unique to each mRNA species would be translated. Such a model would predict three things: first, that the coding capacity of each mRNA would be determined by the difference in size between that RNA and the next smaller species; second, that there would be one primary translation product per mRNA; and third, that the primary translation products would not overlap. Our studies of IBV proteins and the sequence relationships among them (L. Burgess, S. Linesch, and S. I. T. Kennedy, manuscript in preparation) are in agreement with this model. We have identified six virion proteins comprising a large glycoprotein (GP84/90), a smaller glycoprotein (GP31), a 51,000-dalton nucleocapsid phosphoprotein, two other major proteins (P36 and P23), and a minor protein (P28). (Each protein is named according to its apparent molecular weight in kilodaltons as determined by polyacrylamide gel electrophoresis.) Our observations suggest that IBV structural proteins are translated from monocistronic mRNA's: we have been unable to identify a precursor to any of these proteins (i) in pulse-chase experiments, (ii) by use of amino acid analogs, or (iii) by using the protease inhibitor tolylsulfonyl phenylalanyl chloromethyl ketone to interfere with proteolytic cleavage. In vitro translation studies will be necessary to determine the coding assignments for the IBV mRNA's.

Recently Siddell et al. (15) described in vitro translation of intracellular RNA species isolated from cells infected with the murine coronavirus JHM. One pertinent result from this report is that there appear to be two mRNA species sedimenting at 17S and 19S. In vitro translation of the 17S RNA yields the 60,000-dalton (60K) nucleocapsid protein (the predominant JHM protein in infected cells), whereas translation of the 19S RNA produces a 23K protein also seen in infected cells and virions. If the 17S and 19S RNA species correspond to IBV intracellular RNAs A and B, which would be congruent with the sedimentation coefficients, the translation results would agree with a nonoverlapping translation scheme, with the two RNAs of similar size coding for proteins which greatly differ in size. Thus, the avian and murine coronaviruses appear to utilize multiple subgenomic monocistronic mRNA's. Both the number of mRNA

species and the monocistronic nature of the subgenomic mRNA's distinguish the coronaviruses from other positive-stranded viruses.

As described above, the positive-stranded viruses which make use of multiple mRNA's (coronaviruses, alphaviruses, and TMV) all conform to the same pattern, with subgenomic mRNA's mapping to the 3' end of the genome. A subgenomic RNA has been reported for the caliciviruses (1), and it will be interesting to see whether this RNA also fits the pattern. Whether this scheme reflects evolutionary relationships among the positive-stranded viruses or a common response to a constraint imposed by the cell upon the multiplication strategy of the viruses is not clear. Perhaps a better understanding of the mechanisms of transcription and replication utilized by these viruses will provide the answer.

ACKNOWLEDGMENTS

This work was supported by National Science Foundation grant PCM 77-19388 and Public Health Service grant RO1AI 15087 from the National Institutes of Health, both to S.I.T.K. D.S. is the recipient of Public Health Service cell and molecular biology training grant GM07313 from the National Institutes of Health.

LITERATURE CITED

1. **Black, D. N., J. N. Burrough, T. J. R. Harris, and F. Brown.** 1978. The structure of calicivirus RNA. Nature (London) **274**:614–615.
2. **Brzeski, H., and S. I. T. Kennedy.** 1977. Synthesis of Sindbis virus nonstructural polypeptides in chicken embryo fibroblasts. J. Virol. **22**:420–429.
3. **Brzeski, H., and S. I. T. Kennedy.** 1978. Synthesis of alphavirus-specified RNA. J. Virol. **25**:630–640.
4. **Clegg, C., and I. Kennedy.** 1975. Translation of Semliki-Forest-Virus intracellular 26-S RNA. Characterization of the products synthesized *in vitro*. Eur. J. Biochem. **53**:175–183.
5. **Clegg, J. C. S., and S. I. T. Kennedy.** 1974. Polyadenylic acid sequences in the virus RNA species of cells infected with Semliki Forest virus. J. Gen. Virol. **22**:331–345.
6. **Hunter, T. R., T. Hunt, J. Knowland, and D. Zimmern.** 1976. Messenger RNA for the coat protein of tobacco mosaic virus. Nature (London) **260**:759–764.
7. **Jacobson, M. F., and D. Baltimore.** 1968. Polypeptide cleavages in the formation of poliovirus proteins. Proc. Natl. Acad. Sci. U.S.A. **61**:77–84.
8. **Kennedy, S. I. T.** 1976. Sequence relationships between the genome and the intracellular RNA species of standard and defective-interfering Semliki Forest Virus. J. Mol. Biol. **108**:491–511.
9. **Lamb, R. A., P. W. Choppin, R. M. Chanock, and C.-J. Lai.** 1980. Mapping of the two overlapping genes for polypeptides NS_1 and NS_2 on RNA segment 8 of influenza virus genome. Proc. Natl. Acad. Sci. U.S.A. **77**: 1857–1861.
10. **Lomniczi, B., and I. Kennedy.** 1977. Genome of infectious bronchitis virus. J. Virol. **24**:99–107.
11. **MacNaughton, M. R., and M. H. Madge.** 1977. The characterization of the virion RNA of avian infectious bronchitis virus. FEBS Lett. **77**:311–313.
12. **Meinkoth, J., and S. I. T. Kennedy.** 1980. Semliki Forest virus persistence in mouse L929 cells. Virology **100**:141–155.
13. **Robb, J. A., and C. W. Bond.** 1979. Coronaviridae, p. 193–247. *In* H. Fraenkel-Conrat and R. R. Wagner (ed.), Comprehensive virology, vol. 14. Plenum Publishing Corp., New York.
14. **Schochetman, G., R. H. Stevens, and R. W. Simpson.** 1977. Presence of infectious polyadenylated RNA in the coronavirus avian bronchitis virus. Virology **77**:772–782.
15. **Siddell, S. G., H. Wege, A. Barthel, and V. Ter Meulen.** 1980. Coronavirus JHM: cell-free synthesis of structural protein p60. J. Virol. **33**:10–17.
16. **Stern, D. F., and S. I. T. Kennedy.** 1980. Coronavirus multiplication strategy. I. Identification and characterization of virus-specified RNA. J. Virol. **34**:665–674.
17. **Walseth, T. F., and R. A. Johnson.** 1979. The enzymatic preparation of [α-^{32}P] nucleoside triphosphates, cyclic [^{32}P] AMP, and cyclic [^{32}P] GMP. Biochim. Biophys. Acta **526**:11–31.
18. **Watkins, H., P. Reeve, and D. J. Alexander.** 1975. The ribonucleic acid of infectious bronchitis virus. Arch. Virol. **47**:279–286.